The Performance Prediction and Energy Saving Evaluation for the Retrofit of a Gate Rudder System on a General Cargo Vessel using CFD Procedures

Kurt Mizzi[1*], Mariana Zammit Munro[1], Ahmet Gurkan[2], Batuhan Aktas[2], Mehmet Atlar[2], Noriyuki Sasaki[2]

[1]Naval Architectural Services Ltd., Research, Development & Innovation Dept., Paola, Malta
[2]University of Strathclyde, Naval Architecture, Ocean and Marine Engineering, Glasgow, United Kingdom

Abstract: The path to climate neutrality by 2050 has incentivised policymakers to introduce regulatory measures and social pressures in the marine industry to accelerate the development of energy saving technologies and the optimisation of ship propulsion performance to minimise the consumption of fuel. The Gate Rudder System (GRS) is a novel energy saving and manoeuvring device that has successfully demonstrated the reduction of fuel consumption and emissions when installed on newbuilt ships that operate in coastal regions. The GATERS project, funded by the EC EU H2020 programme (ID: 860337), aims to demonstrate the retrofit application of the GRS on ships and is evaluating the retrofit on a general cargo vessel from a holistic point of view, including structure, installation, fabrication, experimental and virtual tank testing. The project brings together leading experts in computational fluid dynamics to identify and implement the best practices to accurately predict the performance of the Gate Rudder System using numerical procedures. This paper provides an overview of the different CFD methods, solvers and approaches that were utilised and fine-tuned to capture the benefits of the GRS and improve ship performance.

Keywords: Gate Rudder System, Virtual Tank Testing, CFD, Numerical Performance Prediction, Energy Saving.

1 INTRODUCTION

The Gate Rudder System (GRS) is an emerging technology in the marine industry that has initially proven a reduction in power requirements as well as improvements in manoeuvring performance, thus offering a solution to the industry for a remarkable reduction in fuel consumption and reduced environmental impact. To further demonstrate and exploit its "Retrofit" potential, technology experts, prime stakeholders, policymakers, and suppliers have come together to collaborate, investigate and study the technology further.

The aim of the GATERS project is to design, manufacture and install a retrofit Gate Rudder System (GRS) on a general cargo vessel and demonstrate the effectiveness of the retrofit technology through sea trials and voyage monitoring (GATERS 2021). Additional goals of the GATERS project are to exploit the potential feasibility, benefits and impact of retrofitting the Gate Rudder System (GRS) across the range of European Short Sea Shipping (SSS) operations or its implementation and impact through wider ship types at the concept exploration level, including the Oceangoing Shipping (OS) operations. The consortium consists of 18 partners across Europe, all having the necessary and complementary expertise to carry out the tasks, disseminate and exploit the project (EU 2021). The GATERS Innovation Action Project is sponsored by the EC H2020 Programme (ID: 860337) with an independent aim and objectives. The project has an official sub-license agreement with Wartsila Netherlands BV to utilise the Gate Rudder Patent (EP 3103715) for specific retrofit projects of vessel sizes below 15000 dwt.

The consortium consists of a dedicated CFD team dedicated to the development of accurate numerical performance prediction procedures for the General Cargo vessel with the current conventional rudder as well as the retrofitted Gate Rudder.

This paper showcases the numerical modelling practices adopted by two of the partners, Naval Architectural Services Ltd. (NAS) and University of Strathclyde (USTRATH) with the aim of accurately predicting the performance of the Gate Rudder System whilst also demonstrating and exploiting the benefits of the technology.

The initial step of the investigation was to validate the different numerical methods by comparing results to experimental benchmark data. Once verified, the study then moved on to analysing the performance of the Gate Rudder System at various speeds at full-load condition. The results indicated average savings of around 7.90% for the different conditions.

2 BACKGROUND

Energy saving devices may be defined as mechanisms that reduce power demand by improving losses in the propeller-hull system (Terwisga 2013). The losses generally

* *Corresponding author e-mail: kurt.mizzi@nas.com.mt*

considered are rotational and axial propeller energy losses, which, if reduced, also lead to lower carbon dioxide emissions – working towards the IMO strategy to reduce GHG emissions from shipping by at least 50% by 2050 compared to 2008 (Spinelli, et al. 2022).

The principle behind the energy saving device being investigated, the Gate Rudder System (GRS), is the presence of two asymmetric rudders at each side of the propeller with the functionality of a ducted propeller. The duct effect of the system provides increased propulsive efficiency and the ability to rotate both rudders, resulting in improved manoeuvrability and seakeeping properties (Sasaki, et al. 2018). Besides the economic advantages provided by the GRS, the safety and habitability of the ship are also improved. Regarding economic gain, the GRS allows for higher propulsive efficiency, an increase of cargo space and a reduction of ship length through the elimination of the conventional rudder. Safety is also improved as the GRS is superior to the conventional rudder in terms of stopping ability, manoeuvrability, berthing performance in crabbing mode and also through reduction of the ship's rolling motion. Moreover, considering the comfort of crew and passengers aboard, the GRS is beneficial as it reduces the propeller-induced noise and hence the system vibration (Turkmen, et al. 2016).

The original purpose of the GRS was to improve the manoeuvrability of Japanese coastal vessels that required tighter control of ships in their transverse motions at ports. The GRS was first applied on the coastal container "Shigenobu", and the vessel's performance was compared to that of her sister ship "Sakura", fitted with a conventional rudder system. The results obtained from sea trials indicated that Shigenobu was 14% more efficient at the design speed than Sakura. Moreover, it was found that the gain in service from employing the GRS can be as high as 30% in rough seas (Sasaki et al., 2020).

In recent years, several numerical and experimental studies have been carried out to determine the feasibility of the GRS. Turkmen et al. (2016) carried out a series of experiments at the Emerson Cavitation Tunnel in the UK to obtain open water propeller data, measure and compare the gate rudder forces with a conventional rudder system (Turkmen, et al. 2016). In conjunction with the model-scale experiments, CFD analysis were conducted to investigate the effect of the full-scale GRS on the flow field at the stern. The results showed that there was an increase in thrust by 10% when the gate rudder was located closer to the propeller plane (at 1.25R in comparison to 1.5R). Turkmen et al. (2016) also performed a cost effectiveness study, where the authors found that the Return on Investment (ROI) for the GRS installed on a new ship would be between 0.56 and 1.18 years, indicating a period of less than a year for most of the scenarios considered. The authors describe a new powering performance prediction technology, the "Fine powering performance prediction technology", that has been developed particularly for ship hulls incorporating Energy Saving Devices (ESDs), for instance, the GRS. The concept is based on the use of a reasonably large model at a relatively high Reynolds number to capture the complex interaction between the model hull, propeller and rudder and more accurately extrapolate the results obtained. Turkmen et al. (2016) found that due to the favourable thrust of the gate rudder, resistance tests revealed a reduction in the resistance of about 1-3%, which is equal to the reduction in hull resistance in the absence of a conventional rudder. Moreover, self-propulsion tests with the GRS revealed 4-8% higher (1-t) value compared to the conventional rudder and open water data for the GRS also presented 15-25% higher (1-w) values (Turkmen, et al. 2016).

Further investigation of the GRS using CFD was conducted by Tacar et al. (2020), who compared experimental and virtual towing tank tests results for full load and sea trial load conditions, with the gate rudder, conventional rudder and with the bare hull (Tacar et al., 2020). Two model sizes were investigated, both experimentally and numerically, of dimensions 2 m and 5 m. For the CFD analysis, the full load condition was investigated, and the realisable k-ε turbulence model was used. The effective power of the GRS was estimated from the experiment, and the CFD simulations and the results were found to be very similar, with the difference between them amounting to just over 1%.

Tacar et al. (2020) performed an open water test for the GRS using the Moving Reference Frame (MRF) method for propeller modelling, which showed very good agreement with the experiment results. They found that as the ship speed increases, the advantageous effect of the GRS also increases, compared to the conventional rudder case at the sea trial condition (Tacar et al., 2020). Moreover, the authors state that at a service speed of 15 knots, the ship fitted with the GRS requires approximately 17% less brake power in comparison to that employing the conventional rudder system. Tacar et al. (2020) then proceeded to extrapolate the experimental model results to full scale using the ITTC 1978 method. The authors found that, with regard to scale effects, the smaller model size overpredicts, while the larger model underpredicts the power requirement, compared to sea trial measurements (Tacar et al., 2020).

ESDs are challenging to evaluate by means of model test results and also during sea trial measurements. Moreover, the issue of scaling arises and leads to improper extrapolation of model test results, causing uncertainties when determining the performance of such devices (Mizzi, et al. 2015). In particular, since ESDs are generally fitted within the boundary layer of the hull, direct extrapolation to full scale conditions is problematic due to the strong viscous effects occurring in the region (Mizzi, et al. 2017).

Moreso, for the GRS, the scale effect is also a topic of concern, as mentioned by Tacar et al. (2020) and further studied in depth by Sasaki et al. (2019), who explored the reasons behind this phenomenon and proposed a new correction procedure.

Sasaki et al. discovered that the resistance of the GRS measured in model tests was 5 to 10 times that of the full-scale results (Sasaki & Atlar, 2019). While the full-scale trials of Shigenobu presented 14% energy savings, the conventional prediction method did not present any gain for the GRS. The authors noted that in the model scale, the GRS experiences laminar flow over the appendages in the stern region, even with turbulence stimulators, as suggested by the ITTC 1978 procedure. Conventional rudders operate in the propeller slipstream, where the accelerated flow suppresses laminar flow separation and therefore do not experience this issue (Sasaki & Atlar, 2019). In fact, other studies have found that ESDs tend to be more efficient at full scale than model scale (Kawamura, Ouchi and Nojiri 2012), (Hansen, Dinham-Peren and Nojiri 2011).

Consequently, the scale effect of the GRS is significantly larger than that of the conventional rudder. Therefore, Sasaki et al. (2019) proposed a correction procedure based on the semi-empirical approaches supported by model and full-scale data. The recommendation by Sasaki et al. (2019) is to divide the measured propeller advance speed, based on the thrust identity, into two components – a different scaling method being applied to each component. However, the authors state that this study would greatly benefit from additional studies, incorporating CFD, systematic model tests and also full-scale trials (Sasaki & Atlar, 2019).

3 GEOMETRY

3.1 Hull & Propeller

The target vessel is a multi-purpose 90m dry cargo ship of 5650 DWT that is equipped with a 5 bladed fixed pitch propeller. The original propeller was initially manufactured to be 3.6m but was later cropped to 3.42m following the sea trials. The hull and propeller characteristics can be found in Table 1 and Table 2.

A 6m hull model and corresponding model propeller were manufactured for experimental testing purposes. Towing tank tests were carried out at various speeds, both at full and trial draught conditions, in both towing and propelled arrangements. The tests were also replicated with the retrofitted Gate Rudder System that was designed and fine-tuned to the form of the vessel. The experimental data was then used as benchmark data for validation and verification purposes of the numerical methods.

Table 1. Hull Characteristics

Parameter	Symbol	Units	Ballast Load	Full Load
Length overall	L_{OA}	*m*	89.95	
Length between perp.	L_{BP}	*m*	84.95	
Breadth	B	*m*	15.4	
Draught (midship)	T	*m*	3.3	6.45
Draught (AP)	T_A	*m*	3.8	6.45
Draught (FP)	T_F	*m*	2.8	6.45
Displacement	Δ	*t*	3607	7241
Block coefficient	C_B	--	0.818	0.84

Table 2. Propeller Characteristics

Parameter (Original / Modified)	Symbol	Unit	Value
Propeller Diameter	D	*m*	3.60 / 3.42
Blade Number	Z	--	5
Pitch Diameter Ratio	P/D	--	0.79
Blade area ratio	BAR	--	0.66 / 0.61
Skew	--	*mm*	26.05
Rake	--	*mm*	5.5

Both the hull and propellers were developed in 3D digital format. It was ensured that the geometry was developed to be free of errors to prevent any issues in the meshing process. Furthermore, the hull form characteristics were verified and compared to the hydrostatics from the stability book to ensure accuracy and precision.

3.2 Gate Rudder System

Similarly, the Gate Rudder System was designed in a 3D format, as shown in Figure 1. This followed an in-house design procedure whereby the wake characteristics of the naked hull were initially analysed, and the Gate Rudder blades and propeller design fine-tuned to optimise the angle of attack of the wake flow on the Gate Rudder System.

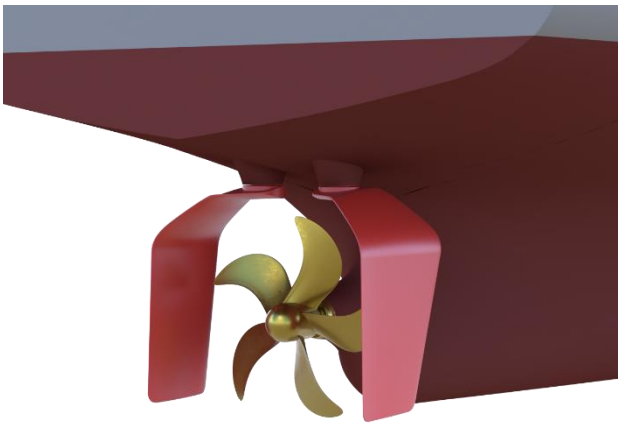

Figure 1. Geometry

3.3 Ship Conditions

For this numerical study, the performance of the retrofitted GRS on the target vessel was analysed at 3 different speeds at full-load conditions. For each operating condition, the vessel was analysed in a naked hull condition (no appendages), towing condition (appendages and no propeller) and self-propelled condition (appendages and propeller).

4. METHODOLOGY

4.1 Numerical Modelling

Both NAS and USTRATH adopted similar approaches for their numerical methods with key differences and models to provide a basis for investigation and discussion. Numerical details and differences are clearly highlighted in the following section.

Both entities used the commercial CFD solver, STAR-CCM+®, to model the multiphase flow using Unsteady Reynold Averaged Navier-Stokes (URANS) equations to simulate a three-dimensional environment. A Volume of Fluid (VOF) method was used to model the free surface effects. With regard to the turbulence model, NAS made use of the Reynolds Stress Model (RSM), whereas USTRATH made use of the realisable k-ε model.

All the studies were carried out in calm water conditions allowing the vessel to pitch or heave. For all the models, the all-y+ wall treatment model was used with the appropriate blending of the prism layer cells to the near domain cells. This is a hybrid approach that allows high-y+ wall treatment for coarse meshes and low-y+ wall treatment for fine meshes. The high-y+ wall treatment adopts the wall-function type approach which assumes that the near-wall cell lies within the logarithmic region of the boundary layer. The near-wall cell centroid must be situated in the logarithmic region of the boundary layer (y+>30). Meanwhile, the low-y+ wall treatment is suitable only for low-Reynolds number turbulence models where the viscous sublayer is properly resolved. This method considers no explicit modelling assumptions and is generally used if the mesh is fine enough for y+ to be approximately 1 or less than 5. NAS have developed their mesh in such a way that that hull is treated using wall functions (y+>30) and the appendages, such as the Gate Rudder System, properly resolved with y+ values smaller than 5. Meanwhile, USTRATH have maintained a y+ lower than 1 on both the hull and appendages, as can be seen in Figure 2.

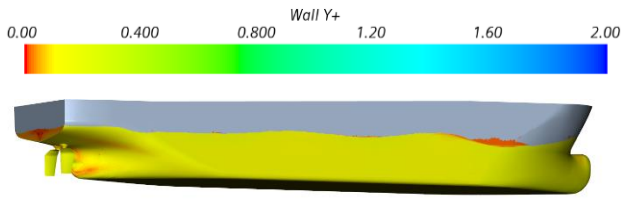

Figure 2. Y+ Distribution on Hull

An implicit unsteady time marching scheme together with a Finite Volume Method (FVM) approach was carried out to treat temporal and spatial discretisation. The time step for all simulations were set to provide adequate convective courant numbers.

The accurate representation of ship geometry is very important as this dictates the flow behaviour. The surface mesh was generated using fine triangulated faces producing detailed geometry, and the volume mesh was developed using the automatic grid generation tool producing an unstructured grid. Mesh refinements have been applied at appropriate critical locations of high gradients to capture the flow behaviour accurately.

For all the simulations, a velocity flow field condition was specified at the inlet boundary and a pressure field for the outlet boundary. All the other boundaries were set with the appropriate physics. The ship geometry was specified with a non-slip wall allowing boundary layer generation. On the other hand, the bottom boundary was placed far enough below the water level to avoid any shallow water effects. Wave damping was also applied to the inlet, outlet and side boundaries, preventing wave reflections.

Furthermore, the propeller behaviour was simulated using the virtual disk feature integrated within Star-CCM+®, commonly known as the actuator disk that makes use of a user-defined momentum source method. More specifically, the body force propeller method was utilised to simulate the propeller's action. This model approach generates a momentum source considering the propeller's geometrical and open water performance characteristics. The distribution of the axial and tangential forces of the propeller and its effect on the flow is calculated. The integration of these forces over the disk gives the thrust and torque of the propeller, which are available for coupling with the hull.

Since the actuator disk does not consider the physical model of the propeller, propeller induced velocities are not accounted for. To tackle this matter, an expert property known as the "Induced Velocity Correction" can be enabled that essentially follows a predictor corrector approach that modifies the local advance ratio and source terms as described in (Neitzel, et al. 2015).

The Body Force Propeller Method requires the definition of the inflow specification of the virtual disk, which in our case, is calculated from the flow field of the vessel. The virtual disk model uses the inflow information for the computation of the advance ratio that is then used to determine the operating point from the propeller open water characteristics curve. In order to establish the self-propulsion point of the vessel such that there is no acceleration/deceleration, the operating point is defined by indicating that the propeller thrust needs to be equal to the ship resistance. The operating point of the propeller is automatically varied until this condition is met.

4.2 Verification & Validation

In order to showcase and justify consistency and reliability of the numerical solver, verification and validation procedures were carried out. The validation and verification studies involved carrying out a mesh refinement study for the conditions with the highest loads and speeds for the model scale condition assumed to be 1:14 of the full-scale ship. Results were processed to ensure validation and verification and tabulated in the standard format/template to allow easy comparison between NAS and USTRATH.

The verification studies were carried out to demonstrate and ensure the capability of the numerical models using the Grid Convergence Index (GCI) that is based on the Richards Extrapolation (L. F. Richardson 1911, Richardson and Gant 1927) to calculate the discretisation error estimates as described by Celik et al. (2008).

The apparent order of the method, p, is calculated using Eqs. (1) to (3), where r_{21} and r_{32} are refinement factors, $\emptyset_k$ is the CFD output parameter (resistance, thrust, torque and RPM) and $\varepsilon_{21}$and ε_{32} represent the difference between the results obtained from grids 1 (fine) and 2, and 2 and 3 (coarse), respectively. For this study, the refinement ratios were selected to be $\sqrt{2}$ (r_{21}, r_{32}) for NAS and 2.3 (r_{21}) and 1.7 (r_{32}) for USTRATH.

$$p = \frac{1}{ln(r_{21})} \left| ln|\varepsilon_{32}/\varepsilon_{21}| + q(p) \right| \quad (1)$$

$$q(p) = ln\left(\frac{{r_{21}}^p - s}{{r_{32}}^p - s}\right) \quad (2)$$

$$s = 1 \cdot \text{sign}\left(\frac{\varepsilon_{32}}{\varepsilon_{21}}\right) \quad (3)$$

The extrapolated values are obtained by Eq. (4).

$$\emptyset^{21}{}_{ext} = \frac{({r_{21}}^p \emptyset_1 - \emptyset_2)}{({r_{21}}^p - 1)} \quad (4)$$

The approximate and extrapolated errors are calculated using Eqs. (5) and (6), and the Grid Convergence Index between the two finest grids (GCI_{21}) is given by Eq. (7).

$$e_a{}^{21} = \left|\frac{\emptyset_1 - \emptyset_2}{\emptyset_1}\right| \quad (5)$$

$$e_{ext}{}^{21} = \left|\frac{{\emptyset_{ext}}^{12} - \emptyset_1}{{\emptyset_{ext}}^{12}}\right| \quad (6)$$

$$GCI^{21}{}_{fine} = \frac{1.25\, {e_a}^{21}}{{r_{21}}^p - 1} \quad (7)$$

Since the angle of attack of the flow to the gate rudder profile is considered crucial to the performance of the technology, NAS has also investigated the accuracy of their numerical method when it comes to wake prediction by comparing it with the experimental wake data. The velocities inside the wake were first processed to initially compare the contours and then compare the velocity distribution along different radial profiles to produce the wake plots for comparison and analysis.

4.3 Computational Set Up

The resource and computational infrastructure set-up is very similar for both partners (NAS and USTRATH), whereby the pre-processing and simulation set-up were configured on office computers using the Star-CCM+® software. In order to run the simulations, due to the high computational requirements, both partners make use of a High-Performance Computer (HPC) cluster to have access to more nodes and cores that can be utilised simultaneously. The information is uploaded onto the HPC via remote access and runs via a scheduler. The computational set-up is portrayed in Figure 3.

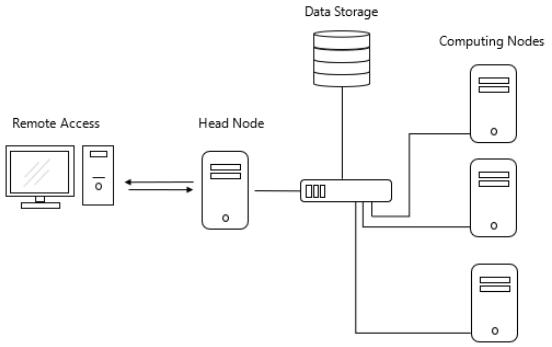

Figure 3. Computational Set-up

5. RESULTS & DISCUSSION

5.1 Verification & Validation

Verification

The GCI was used as a metric of comparison between the three grids of varying grid densities. Table 3 displays the GCI^{21} values for comparison between the turbulence models employed by USTRATH and NAS for the simulations analysing the GRS at full-load draught, in towing and self-propulled conditions. It should be noted that the simulations performed by USTRATH, used the realisable k-ε model, while NAS used the RSM, both running the condition of Fr = 0.225, equivalent to the speed condition of 13 knots.

Table 3. Verification Study - Turbulence Model Comparison

	Realisable k-ε	***RSM***
	GCI^{21} %	
R_T	0.33	0.07
T	0.33	0.54
Q	0.28	0.45
rps	0.09	0.04

As presented in Table 3, for the resistance in towing condition (R_T), the RSM and realisable k-epsilon turbulence models both produced converged results with GCI^{21} values of 0.07% and 0.33% respectively. With regards to the parameters measured in self-propelled conditions (T, Q, rps), both the realisable k-epsilon model and RSM turbulence produced converged results, with the GCI^{21} values ranging from 0.04% to 0.54% for the various parameters.

The fine mesh configurations for both numerical models, featured significantly high cell numbers requiring substantial computational power. Therefore, it was not considered feasible to carry out the study using such mesh sizes. Since the medium mesh configurations produced very similar results to the fine mesh models, it was decided, by both partners, to carry out the validation comparison and GRS impact study using the medium grid size characteristics.

Validation

For validation with experimental (EFD) results, the percentage error between the EFD and CFD results were computed for the simulations analysing the GRS at full-load draught, in towing and self-propulled conditions. As portrayed in Table 4, for the resistance in towing condition (R_T), the realisable k-ε model produced more accurate results in comparison to experimental data, with a percentage error of 0.15%. However, for the parameters measured in self-propulsion conditions (T, Q, rps), the RSM and realisable k-epsilon model yielded similar results with values ranging from 1.43% to 3.76% across the different paramaters.

In summary, the verification study produced satisfactory results that in most cases reflected monotonic convergence for both the realisable k-ε and RSM turbulence models. Moreover, the validation study for both turbulence models revealed good agreement with experimental results.

Table 4. Validation Study - Turbulence Model Comparison

	Realisable k-ε	***RSM***
	Error %	
R_T	0.15	2.79
T	3.42	2.88
Q	3.76	3.62
rps	1.43	2.29

5.2 Wake Validation

Wake Contours

The towing simulation with GRS computed with the RSM turbulence model was further post-processed to validate and compare the wake behaviour at the propeller plane position with the available EFD data. As displayed in Figure 4, at first impression, the wake behaviour is similar. However, the CFD output indicates a symmetrical wake, whereas the experimental wake is not symmetrical. The matter is currently being investigated.

Experimental Processed Data **CFD Output (NAS)**

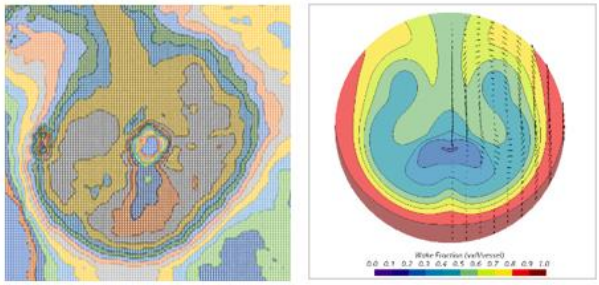

Figure 4. Wake Contour Comparison

The analysis then proceeded to compare the velocity distribution of the wake, between the CFD (RSM model) and the EFD tests, along different radial profiles at the propeller plane that led to the developemnt of wake plots, as displayed in Tables 5, 6 and 7.

In general, one can notice the symmetrical behaviour of the numerical Vx wake plots in contrast to the experimental wake behaviour. Trends in wake distribution and velocity profile in the x-direction are sufficiently accurate except near the 180° region (see Table 5). Trends in V_y wake distribution and velocity profile in the y-direction are sufficiently similar to the experimental data. While not conclusive, CFD tends to underpredict the velocity in the y-direction (see Table 6). At the same time, the trends in V_z wake distribution and velocity profile in the z-direction are sufficiently similar to the experimental data, particularly at higher radii (see Table 7).

Wake Plots

Table 5. Wake Profile Comparison - V_x

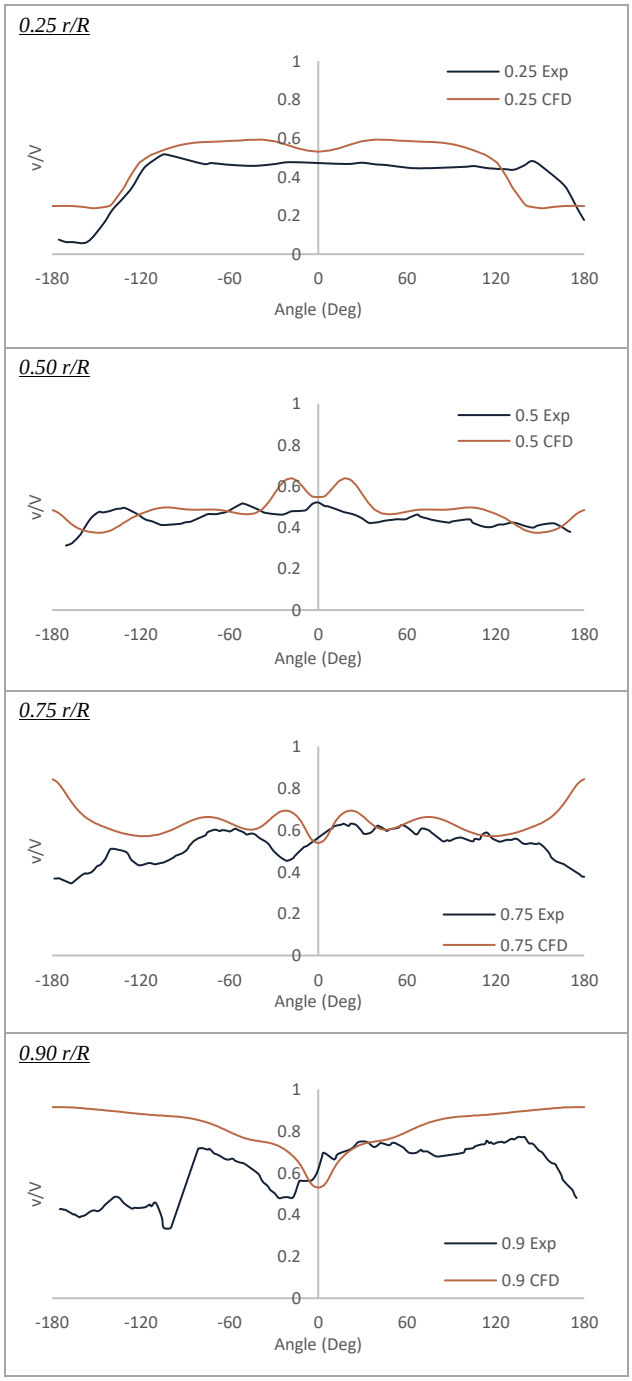

Table 6. Wake Profile Comparison - V_y

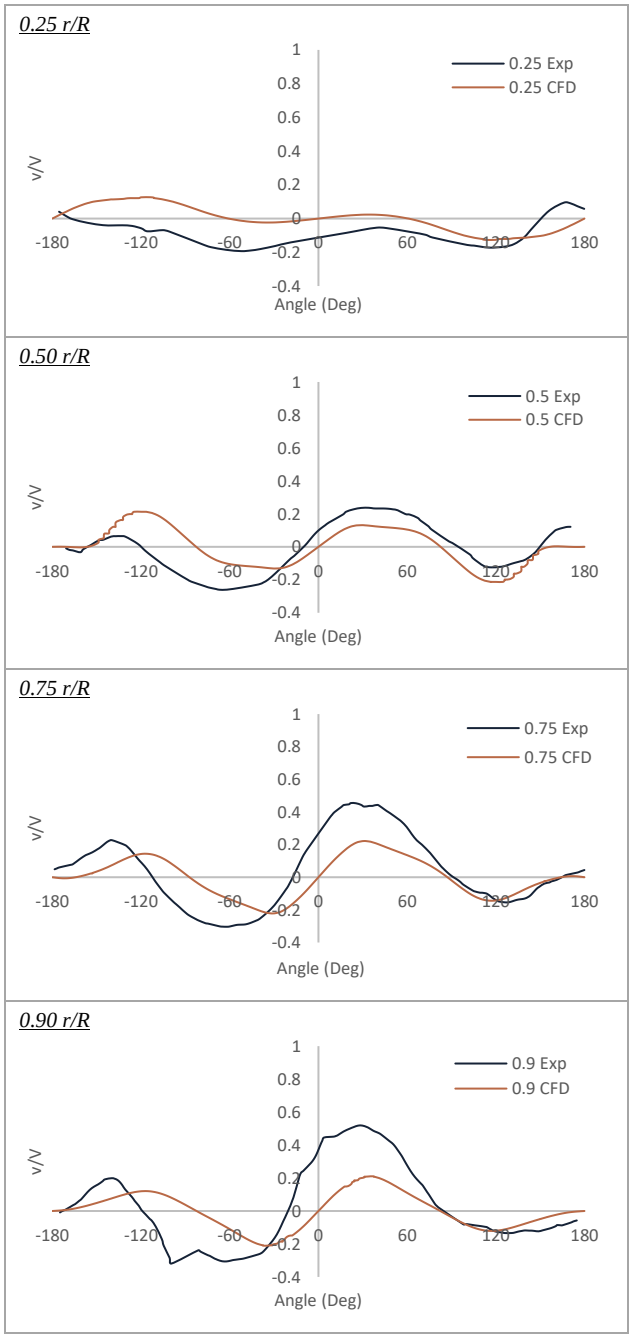

Table 7. Wake Profile Comparison – V_z

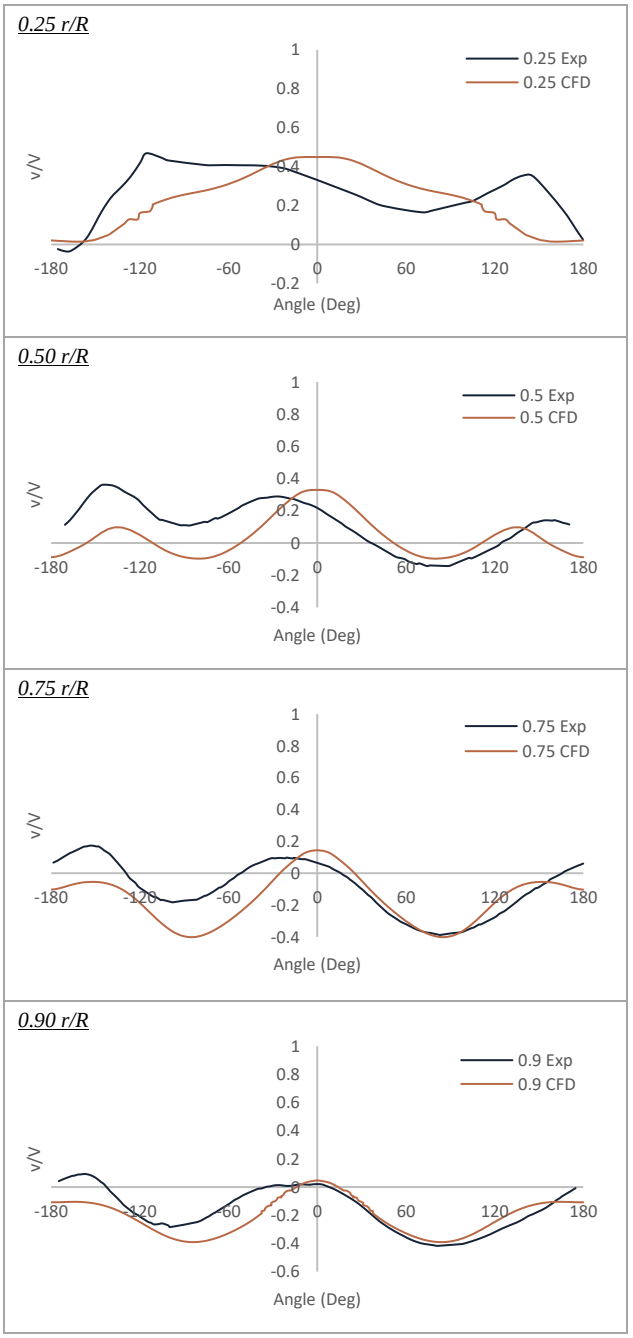

5.3 Gate Rudder Performance

Once the numerical models had been validated and verified for both entities respectively, the same models were then used to compute and predict the performance of the target ship with the conventional rudder system (CRS) as well as the gate rudder system (GRS) at three different speeds (11kts, 12kts and 13kts) at full-load condition. As shown in Figures 5 and 6, it is further reassuring that the performance predictions for the effective power (P_E) as well as the delivered power (P_D) that were conducted by both partners for the three speeds, are exhibiting similar results and trends. It is evident from the effective power (P_E) curves in Figure 5 that the benefits of the GRS over CRS in towing conditions are minor.

NAS results have indicated an average 1% effective power improvement across the three different speeds whilst USTRATH results indicate an average improvement of 0.70%. This is expected as the GRS requires the action of the propeller to exploit its benefits. This is clearly demonstrated in the delivered power (P_D) curves (Figure 6), that indicate an average power improvement of 8.26% across the three speeds by NAS and 7.35% by USTRATH.

The measured data for Resistance, Thrust, Torque and RPM were further processed to compute and compare the propulsive efficiency parameters between the conventional rudder condition as well as the gate rudder system to better understand the reason behind the benefits of the GRS. Results have been tabulated in Table 8.

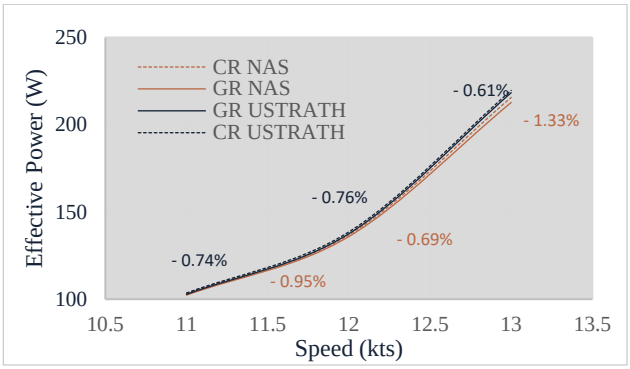

Figure 5. Effective Power Prediction

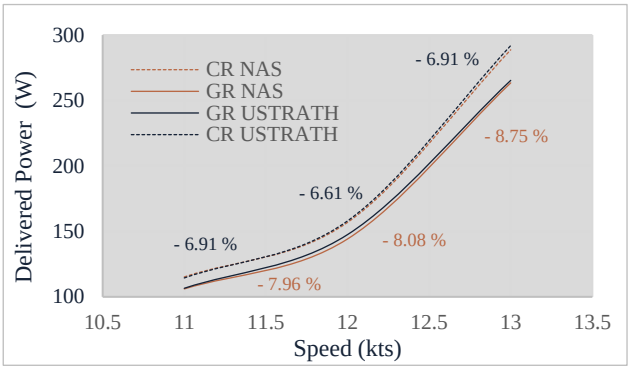

Figure 6. Delivered Power Prediction

Whilst the relative rotative efficiency (η_R) is similar between both rudder types; the hull efficiency is lower for the hull with GRS. This may be explained by the reduction in wake fraction (w_t) across the three different speeds, which is not offset by the decrease in the thrust deduction fraction (t), which leads to a net reduction of hull efficiency.

The Gate Rudder blades produce a thrust (as opposed to the resistance produced by the conventional rudder) in the propelled condition. The result of this added thrust is a reduction in the total ship resistance (R_{sp}), and hence the thrust requirement (T) by the propeller is lower, leading to a lower thrust deduction fraction (t). Since the propeller is required to produce a lower thrust value, it needs to operate at different operating points and higher advance ratios (J). Assuming that the advance velocity is similar for both rudder scenarios, one would expect a reduced rpm value (n) for the GRS condition to produce a higher J value. However, the GRS conditions have produced slightly higher propeller rotation measurments. Therefore, this implies that the advance velocity (V_a) is different between the conditions. As previously stated, 1-w_t is higher across the three speeds for the GRS conditions. This implies that the presence of the Gate Rudder imparts an acceleration to the flow inside the propeller plane. The loss in hull efficiency (η_H) by the GRS conditions, is however, compensated by the enhanced open water efficiency (η_O). This is due to the higher advance ratio of the propeller as can be seen in Figure 7 for one of the speeds.

As seen in Table. 8, the product of all three efficiencies (η_R, η_H, η_O) yields the propulsive efficiency (η_D), indicating a higher efficiency of around 7% across the three speeds (between both NAS and USTRATH) for the GRS retrofitted hull as opposed to the CRS conditions. This improvement, together with the reduction in effective power (PE), leads to the benefits in delivered power (PD) that were previously stated.

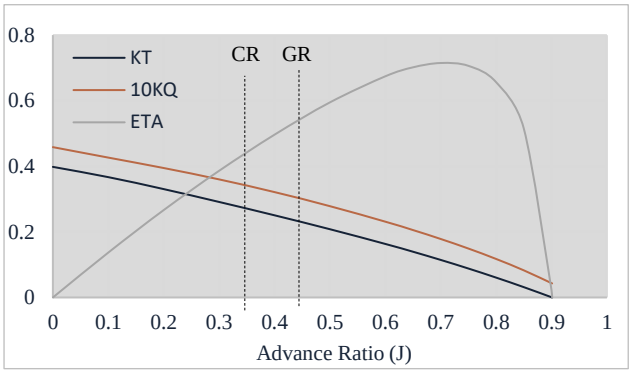

Figure 7. Propeller Open Water Data

Local Flow Analyses

Table 9 presents the hydrodynamic forces (i.e., resistance and/or thrust) measured on the hull and rudder(s) components, both in towing and self-propelled conditions, for the RSM numerical models. A positive (+) force indicates resistance, while a negative (-) force indicates a thrust. The percentages indicate the magnitude of the respective forces in proportion to the total force on the hull and rudder(s).

As shown in Table 9, in the towing condition, the Gate Rudder blades produce a minor resistance force, an average of 1.37% of the total resistance across the three speeds. This is very similar to the resistance produced by the conventional rudder at an average of 1.76% of the total resistance across the three speeds. However, in the self-propelled condition, since the propeller action accelerates the flow and hence alters the angle of attack of the flow favourably on the rudder blades, the Gate Rudder blades

Table 8. Propulsive Efficiency Parameters

		NAS								USTRATH							
	Vs	η_0	w	t	η_H	η_r	η_D	P_E	P_D	η_0	w	t	η_H	η_r	η_D	P_E	P_D
	m/s	--	--	--	--	--	--	*W*	*W*	--	--	--	--	--	--	*W*	*W*
CRS	11	0.48	0.48	0.24	1.45	1.00	0.70	103	115	0.49	0.47	0.24	1.43	1.00	0.70	104	114
	12	0.48	0.47	0.25	1.41	1.00	0.68	137	157	0.49	0.46	0.24	1.41	1.00	0.69	139	158
	13	0.45	0.45	0.23	1.40	1.00	0.63	216	289	0.46	0.44	0.23	1.37	1.00	0.62	220	292
GRS	11	0.59	0.32	0.14	1.27	1.00	0.75	102	106	0.60	0.30	0.13	1.24	1.00	0.74	103	107
	12	0.59	0.31	0.13	1.26	1.00	0.74	136	144	0.60	0.28	0.13	1.22	1.00	0.73	137	148
	13	0.55	0.29	0.15	1.21	1.00	0.67	213	263	0.56	0.27	0.12	1.21	1.00	0.68	218	265

Table 9. Comparison of Simulated Forces on the Hull and Rudder(S)

		Towing			Self-Propulsion				
Gate Rudder System	V	$Hull_T$	GRS_T	RT_T	$Hull_{SP}$	GRS_{SP}	RT_{SP}	FD	T
	kts	*N*	*N*	*N*	*N*	*N*	*N*	*N*	*N*
	11	66.602	1.09	67.692	79.76	-3.65	76.11	15.41	60.7
		98.39%	*1.61%*	*100%*	*104.80%*	*-4.80%*	*100%*	--	--
	12	81.17	1.2	82.37	96.31	-4.45	91.86	17.4	74.46
		98.54%	*1.46%*	*100%*	*104.84%*	*-4.84%*	*100%*	--	--
	13	117.785	1.255	119.04	141.9705	-5.92	136.05	20.76	115.29
		98.95%	*1.05%*	*100%*	*104.35%*	*-4.35%*	*100%*	--	--
Conventional Rudder	V	$Hull_T$	CR_T	RT_T	$Hull_{SP}$	CR_{SP}	RT_{SP}	FD	T
	kts	*N*	*N*	*N*	*N*	*N*	*N*	*N*	*N*
	11	67.04	1.3	68.34	83.963	1.667	85.63	15.02	70.61
		98.10%	*1.90%*	*100%*	*98.05%*	*1.95%*	*100%*	--	--
	12	81.35	1.59	82.94	102.823	1.967	104.79	18.23	86.56
		98.08%	*1.92%*	*100%*	*98.12%*	*1.88%*	*100%*	--	--
	13	118.86	1.78	120.64	149.59	1.77	151.36	18.45	132.91
		98.52%	*1.48%*	*100%*	*98.83%*	*1.17%*	*100%*	--	--

then produce thrust at an average of 4.7 % of the total resistance across the three speeds. In contrast, with an active propeller, the conventional rudder still produces roughly 1.7% of the total resistance across the three speeds The results further indicate that the presence of the GR in propelled condition augments the hull resistance favourably, indicating that the Gate Rudder has a positive influence on the pressure resistance of the hull. Also, as seen in Figure 8, most of the GR geometry produces a thrust in propelled condition except for the horizontal part of the rudder blade at the top producing detrimental performance (i.e. resistance). It is interesting to note that a similar thrust was produced by both blades (PS & SB) even if the propeller's rotational action is not entirely symmetrical.

5.4 Propeller Treatment

Further analyses were carried out by USTRATH to analyse the impact of the numerical propeller treatment methodology on the performance of the GRS. In this particular case, a study was carried out to analyse and compare the difference in GRS performance when using the virtual disk (VD) approach in comparison to the sliding mesh (SM) approach in full-scale conditions. As can be seen in Figure 9, the average rudder forces are similar for both approaches. However, with the rigid body (SM), it can be stated that rudder force characteristics are sensitive to the propeller rotation direction. The rudder forces on the port side are higher since the interaction with the propeller is enhanced due to the related flow vector field.

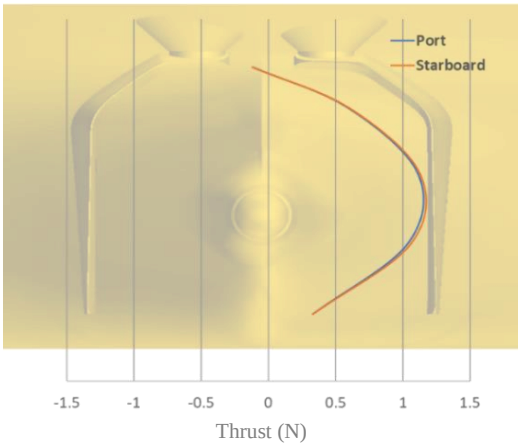

Figure 8. Thrust Blade Profile

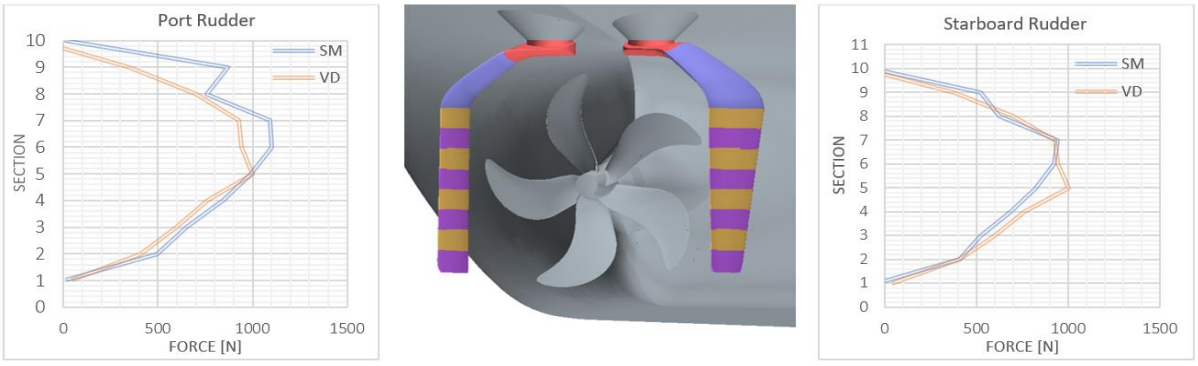

Figure 9. SM vs VD Propeller Treatment Comparison.

6. CONCLUSION

This paper presents the joint effort of two partners of the GATERS project, NAS and USTRATH, who successfully demonstrate the benefits of the Gate Rudder System (GRS) technology using CFD procedures by adopting and investigating different numerical modelling practices. In particular, model scale simulations were carried out using two different turbulence models, and the results obtained were successfully verified and validated. In summary, for most of the CFD simulations, the GCI reflected monotonic convergence, indicating sound results for all conditions. Moreover, the CFD results provided good agreement with experimental data for all conditions.

The numerical performance predictions of the GRS behaviour outlined in this study are in line with similar published literature, which show that the Gate Rudder System is beneficial, particularly due to the reason that the rudder blades produce a thrust and accelerate the wake flow in the propeller plane region thus leading to reduced power demand and fuel consumption. Future work for the GATERS project includes a study, similar to the one outlined in this paper but at full-scale conditions to determine the performance of this GRS in ship-scale conditions.

ACKNOWLEDEGEMENTS

This paper is based on the activities conducted in the collaborative European project GATERS which is an Innovation Action Project funded by the EC H2020 Programme (ID: 860337) with the independent aim and objectives. The project has an official sub-license agreement with Wartsila Netherlands BV to utilise the Gate Rudder Patent (EP 3103715) at specific retrofit projects of vessel sizes below 15000 DWT.

REFERENCES

Celik, I. B., Ghia, U., Roache, P. J., Freitas, C. J., Coleman, H., & Raad, P. E. (2008). 'Procedure for estimation and reporting of uncertainty due to discretization in CFD applications'. *Journal of Fluids Engineering-Transactions of the ASME 078001-078001-4 , 130*((7)).

EU. (2021). *Horizon 2020 - GATE Rudder System as a Retrofit for the Next Generation Propulsion and Steering of Ships*. Retrieved from Horizon Collaboration Network: https://cordis.europa.eu/project/id/860337

GATERS. (2021). *Gaters Project*. Retrieved from https://www.gatersproject.com/

Hansen, H., Dinham-Peren, T., & Nojiri, T. (2011). Model and full scale evaluation of a 'Propeller Boss Cap Fins' device fitted to an afromax tanker. *Second International Symposium on Marine Propulsors.* Hamburg.

Kawamura, T., Ouchi, K., & Nojiri, T. (2012). 'Model and full scale CFD analysis of propeller boss cap fins (PBCF)'. *J. Mar. Sci. Technol.*

Mizzi, K., Demirel, Y. K., Banks, C., Turan, O., Kaklis, P., & Atlar, M. (2017). 'Design optimisation of Propeller Boss Cap Fins for enhanced propeller performance'. *Applied Ocean Research*, 210-222.

Mizzi, K., Kim, M., Turan, O., & Kaklis, P. (2015). 'Issues with energy saving devices and the way forward'. *Shipping in Changing Climates Glasgow.* Glasgow.

Neitzel, J., Pergande, M., Berger, S., & Abdel-Maksoud, M. (2015). 'Influence of the Numerical Propulsion Modelling on the Velocity Distribution behind the Propulsion Device and Manoeuvring Forces'. *Fourth International Symposium on Marine Propulsors* . Austin, Texas.

Richardson, L. F. (1911). 'The approximate arithmetical solution by finite differences of physical problems involving differential equations, with an application to the stresses in a masonry dam'. *Transactions of the Royal Society of London, 210*(459-490).

Richardson, L. F., & Gant, J. A. (1927). 'The deferred approach to the limit'. *Transactions of the Royal Society of London, 226*(636-646).

Sasaki, N., & Atlar, M. (2019). 'Scale Effect of Gate Rudder'. *Sixth International Symposium on Marine Propulsors.* Rome.

Sasaki, N., Kuribayashi, S., Atlar, M., & Steam Co, K. (2018). 'Gate Rudder'. *INT-NAM2018: 3rd International Symposium on Naval Architecture and Maritime.* Istanbul.

Sasaki, N., Kuribayashi, S., Fukazawa, M., & Atlar, M. (2020). 'Towards a realistic estimation of the powering performance of a ship with a gate rudder system'. *Journal of Marine Science and Engineering*.

Spinelli, F., Mancini, S., Vitiello, L., De Carlini, M., & Bilandi, R. N. (2022). 'Shipping Decarbonization: An Overview of the Different Stern Hydrodynamic Energy Saving Devices'. *Journal of Marine Science and Engineering (JSME)*.

Tacar, Z., Sasaki, N., Atlar, M., & Korkut, E. (2020). 'An investigation into effects of Gate Rudder® system on ship performance as a novel energy-saving and manoeuvring device'. *Ocean Engineering*.

Terwisga, T. (2013). 'On the working principles of energy saving devices'. *3rd International Symposium on Marine Propulsors.* Tasmania, Australia.

Turkmen, S., Carchen, A., Sasaki, N., & Atlar, M. (2016). '*A New Energy Saving Twin Rudder System-Gate Rudder'*.